Res Chem Intermed (2018) 44:4519–4531
https://doi.org/10.1007/s11164-018-3401-5

Nano-cellulose/BF_3/Fe_3O_4: a magnetic bio-based nano-catalyst for the synthesis of pyrimido[2,1-*b*]benzothiazoles under solvent-free conditions

Bi Bi Fatemeh Mirjalili[1] · **Fatemeh Aref**[1]

Received: 5 January 2018 / Accepted: 16 March 2018 / Published online: 28 March 2018

Abstract Nano-cellulose/BF_3/Fe_3O_4 is a bio-based and eco-friendly catalyst with high catalytic activity. Easy separation with an external magnet and recyclability without significant loss of its activity are some advantages of this catalyst. Nano-cellulose/BF_3/Fe_3O_4 was characterized by Fourier transform infrared spectroscopy, field emission scanning electron microscopy, transmission electron microscopy, X-ray diffraction, X-ray fluorescence, vibrating sample magnetometry, thermogravimetric analysis, and BET theory. The catalyst was applied for the synthesis of 4*H*-pyrimido[2,1-*b*]benzothiazole derivatives via one-pot condensation of aldehydes, 2-aminobenzothiazol and ethyl acetoacetate, under solvent-free conditions at 100 °C. This method offers several advantages including easy work-up, excellent yields and short reaction time.

Electronic supplementary material The online version of this article (https://doi.org/10.1007/s11164-018-3401-5) contains supplementary material, which is available to authorized users.

✉ Bi Bi Fatemeh Mirjalili
fmirjalili@yazd.ac.ir

[1] Department of Chemistry, College of Science, Yazd University, P.O. Box 89195-741, Yazd, Islamic Republic of Iran

Graphical Abstract

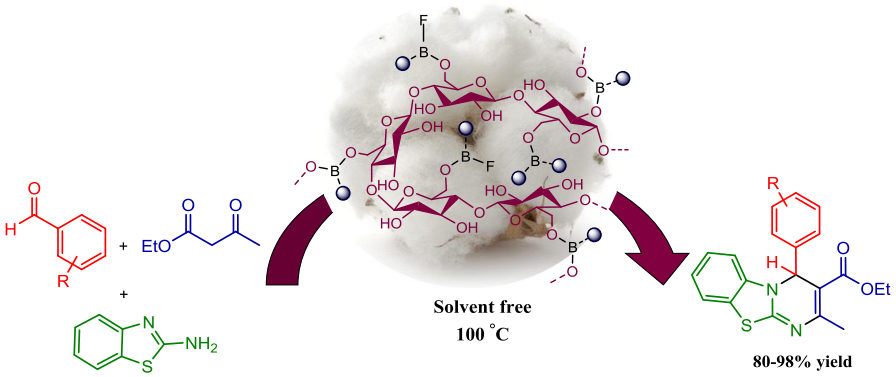

Keywords Nano-cellulose/BF_3/Fe_3O_4 · Bio-based catalyst · Magnetic nano-catalyst · 4*H*-pyrimido[2,1-*b*]benzothiazole

Introduction

Today, many organic reactions are synthesized using acidic catalysts, while liquid acid catalysts are less used due to the difficulty in separation, and their corrosive and highly toxic nature [1]. By bonding liquid acids to an efficient support, they can be converted to solid acid catalysts which lack the problems associated with liquid acid catalysts and play an important role in green chemistry [2].

Nano-cellulose is a unique natural polymer with considerable physical and biological properties such as biocompatibility, biodegradability and low toxicity [3]. It has been used in numerous fields such as medicine [4, 5], electronics [6], tissue engineering [7] and pharmacy [8]. Due to its high surface area, thermal stability, and surface OH groups, it can be used as a suitable support for the preparation of nano-catalysts based on biopolymers [9].

Nano-catalysts with diameters of less than 100 nm are difficult to separate from the reaction mixture and the use of magnetic nanoparticles in the catalyst structure is a logical solution to overcome this problem. Among them, Fe_3O_4 nanoparticles have attracted much attention [10] as they have advantages such as good stability, easy synthesis and functionalization, availability, easy separation and low toxicity [11, 12].

Heterocyclic compounds play a significant role in medicinal chemistry, and among them, pyrimido[2,1-*b*]benzothiazoles show numerous biological activities including antituberculosis [13], antibacterial [14, 15], antiviral [16], antifungal [17–19], antitumor [20], anti-allergic [21], and anti-inflammatory [22, 23], and the inhibition of lung cancer [24].

Numerous methods have been developed for the synthesis of pyrimido[2,1-*b*]benzothiazoles, via three-component condensation of β-keto ester, aromatic

aldehydes and 2-amino benzothiazole. Various catalysts, such as 1,1,3,3-*N*,*N*,*N*′,*N*′-tetramethylguanidinium trifluoroacetate (TMGT) [25], FeF_3 [26], thiamine hydrochloride (VB1) [27], tetrabutylammonium hydrogen sulfate (TBAHS) [28], kaolin [29], acetic acid [30] and $AlCl_3$ [19], have been applied for the preparation of pyrimido[2,1-*b*]benzothiazoles. Some of these catalysts are faced with drawbacks such as long reaction times, low performance, toxicity and lack of recoverability.

In this work, we report on nano-cellulose/BF_3/Fe_3O_4 as a bio-based, magnetic and biodegradable nano-catalyst for the synthesis of 4*H*-pyrimido[2,1-*b*]benzothiazole derivatives via one-pot three-component condensation of ethyl acetoacetate, aromatic aldehydes and 2-amino benzothiazole.

Experimental

General

All compounds were purchased from Merck, Aldrich and Fluka and used without any additional purification. A refrigerated centrifuge (Eppendorf Centrifuge 5417R) was used for the preparation of nano-cellulose. Fourier transform infrared (FT-IR) spectra were run on a Bruker, Equinox 55 spectrometer. A Bruker (DRX-400 Avance) NMR was used to record the ^{1}H-NMR spectra. Melting points were determined by a Buchi melting point B-540 B.V.CHI apparatus and were uncorrected. X-ray diffraction (XRD) patterns were obtained with a Philips Xpert MPD diffractometer equipped with a Cu Ka anode (k = 1.54 Å) in the 2θ range from 10° to 80°. Field emission scanning electron microscopy (FESEM) was carried out on a Mira 3-XMU, and transmission electron microscopy (TEM) using a Philips CM120 with a LaB6 cathode and an accelerating voltage of 120 kV. X-ray fluorescence (XRF) analysis was carried out with a Bruker S4 Explorer instrument. Vibrating sample magnetometry (VSM) measurements were performed by using a vibrating sample magnetometer (Meghnatis Daghigh Kavir, Kashan Kavir, Iran). Brunauer–Emmett–Teller (BET) surface area analysis of the catalyst was carried out with a Micromeritics, Tristar II 3020 analyzer.

Preparation of nano-cellulose from cotton

A sample of 4 g of cotton fibers was washed several times with distilled water, and then to remove other compounds present in the fibers, such as lignin, hemicellulose, wax and organic acids, with 160 ml of 17.5% NaOH solution for 24 h under reflux conditions. After that, the fibers were washed with distilled water several times in order to obtain a neutral pH. Then, to bleach the cotton fibers, 20 ml of sodium hypochlorite solution plus 60 ml of distilled water were added to the cotton fibers under reflux conditions for 2 h. Subsequently, the cotton fibers were again washed with distilled water. In order for acid hydrolysis and the preparation of nano-cellulose, 80 ml of the 35% sulfuric acid aqueous solution was added to the cotton fibers under reflux conditions. After 6–7 h, the resulting suspension was diluted with water, then centrifuged at 4000 rpm. To separate the resulting nano-cellulose from

the acidic solution and to remove any remaining free acid, washing with water and centrifugation were repeated several times.

Preparation of nano-cellulose/BF_3/Fe_3O_4

An amount of 0.5 ml of BF_3 was added dropwise to a mixture of nano-cellulose (0.5 g) in 5 ml of dichloromethane and stirred for 1 h at room temperature. Then, the resulting mixture was filtered and washed with dichloromethane and dried at room temperature. Subsequently, the resulting nano-cellulose/BF_3 with 5 g of Fe_3O_4 nanoparticles were dispersed in 5 ml of dichloromethane under ultrasound irradiation at room temperature for 1 h. Then, the resulting suspension was filtered and washed with dichloromethane and dried at room temperature so that he nano-cellulose/BF_3/Fe_3O_4 catalyst was obtained.

General procedure for synthesis of 4*H*-pyrimido[2,1-*b*]benzothiazole derivatives

Nano-cellulose/BF_3/Fe_3O_4 (0.06 g) as a catalyst was added to a mixture of aromatic aldehyde (1 mmol), ethyl acetoacetate (1 mmol), and 2-aminobenzothiazole (1 mmol). The mixture was stirred at 100 °C. After completion of the reaction (monitored by TLC), the reaction mixture was dissolved in ethanol and the catalyst was separated by an external magnet and reaction mixture was filtered. Then, by adding water to the filtrate, the product appeared.

Results and discussion

In this work, nano-cellulose/BF_3/Fe_3O_4 was prepared in several steps. At first, nano-cellulose was obtained from the acid hydrolysis of cotton. Then, BF_3 was added to the mixture of nano-cellulose and CH_2Cl_2. The OH groups present in the nano-cellulose act as a nucleophile and a B–O–C bond was formed by the interaction between the BF_3 and the OH groups. Then, the resulting nano-cellulose/BF_3 was added to the mixture of Fe_3O_4 nanoparticles/CH_2Cl_2. Some of the fluorine atoms remaining in the BF_3 were replaced by surface OH groups in the Fe_3O_4 nanoparticles, and nano-cellulose/BF_3/Fe_3O_4 was prepared (Scheme 1).

Characterization of the nano-cellulose/BF_3/Fe_3O_4 structure was performed using various techniques such as FT-IR, FESEM, TEM, XRD, XRF, VSM, TGA and BET. The FT-IR spectra of (a) nano-cellulose, (b) Fe_3O_4, (c) nano-cellulose/BF_3/Fe_3O_4 and (d) recovered nano-cellulose/BF_3/Fe_3O_4 are shown in Fig. 1. The FT-IR spectrum of nano-cellulose shows the stretching vibrations of the OH group at 3339 cm^{-1} and the stretching vibrations of the C–O group at around 1059 and 1162 cm^{-1}. In the FT-IR spectrum of nano-cellulose/BF_3/Fe_3O_4, in addition to the above-mentioned bands, the stretching vibrations of the Fe/O bond appears at 560 cm^{-1}. The band at 1371 cm^{-1} displays the stretching vibrations of the B–O bond, indicating that the BF_3 is supported on the nano-cellulose.

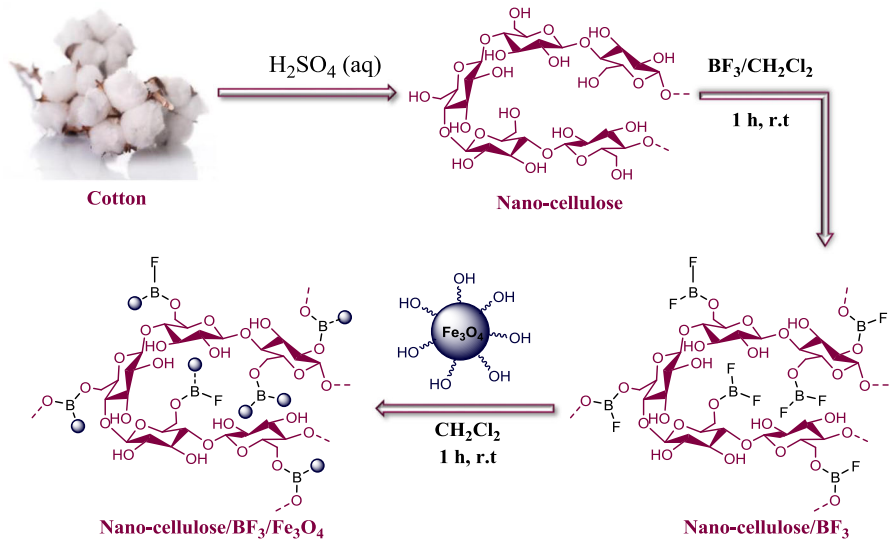

Scheme 1 Preparation of nano-cellulose/BF_3/Fe_3O_4

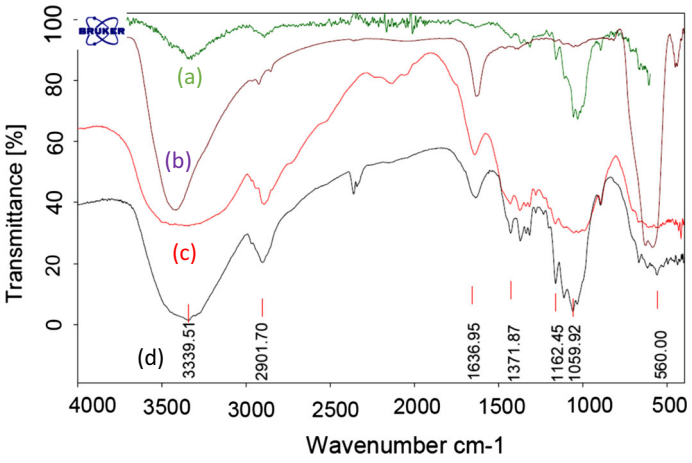

Fig. 1 FT-IR spectra of **a** nano-cellulose, **b** Fe_3O_4, **c** nano-cellulose/BF_3/Fe_3O_4 and **d** recovered nano-cellulose/BF_3/Fe_3O_4

The particle sizes of the nano-cellulose/BF_3/Fe_3O_4 were investigated using FESEM and TEM. The images in Fig. 2 indicate that the nano-cellulose/BF_3/Fe_3O_4 particles are on average about 20 nm.

XRD patterns of nano-cellulose/BF_3/Fe_3O_4 and Fe_3O_4 are shown in Fig. 3. According to the XRD pattern of nano-cellulose/BF_3/Fe_3O_4 (Fig. 3a), signals in 2θ equal to 23° and 13° are related to the cellulose. The signals in 2θ = 30°, 35.5°, 43°, 53.5°, 57° and 62.9° show the existence of Fe_3O_4. Other peaks at around 2θ = 13 and 28 are, it seems, related to the bonding of B on the surface of nano-cellulose.

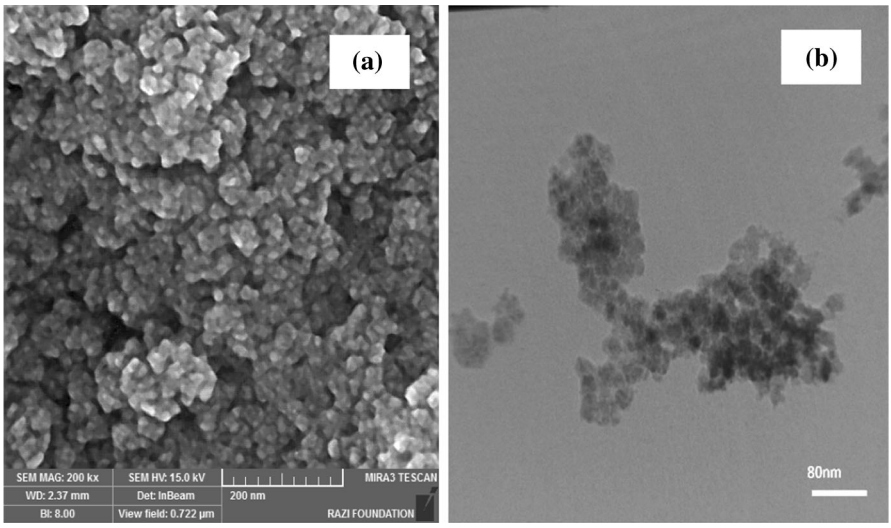

Fig. 2 **a** FESEM image of nano-cellulose/BF_3/Fe_3O_4, **b** TEM image of nano-cellulose/BF_3/Fe_3O_4

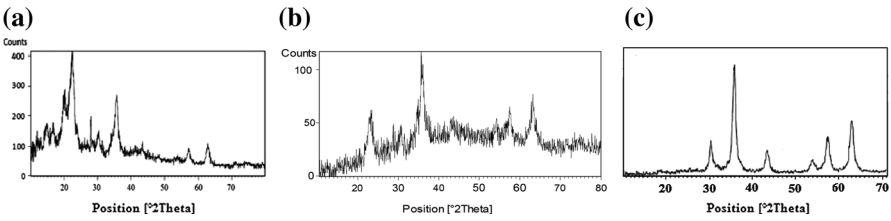

Fig. 3 XRD patterns of the **a** fresh nano-cellulose/BF_3/Fe_3O_4, **b** reused nano-cellulose/BF_3/Fe_3O_4 and **c** Fe_3O_4

The XRF method was used for elemental analysis of nano-cellulose/BF_3/Fe_3O_4. To determine the B:F ratio in the catalyst, the kilo counts per second (KCPS) of elements in the catalyst was compared with the KCPS of elements in the pure H_3BO_3 and NaF (Table 1). The amounts obtained for B and F are 3.496 g (0.32 mol) and 1.112 g (0.059 mol), respectively. Thus, the B:F ratio, in the catalyst is approximately 5:1.

Table 1 Results of XRF analysis of catalyst and standard samples of H_3BO_3 and NaF

Elemental component	Nano-cellulose/BF_3/Fe_3O_4			NH_3BO_3		NaF	
	B%	F%	KCPS	B%	KCPS	F%	KCPS
B	3.496	–	0.5	17.48	2.5	–	
F	–	1.112	1	–		45.25	40.7

The magnetic properties of Fe_3O_4 and nano-cellulose/BF_3/Fe_3O_4 were characterized at 300 K using VSM (Fig. 4). According to the hysteresis loop magnetism, there is no remnant magnetization and also the coercivity value is zero for both samples, which confirms the super-paramagnetic properties of the samples at room temperature. The amounts of saturation magnetization for Fe_3O_4 and nano-cellulose/BF_3/Fe_3O_4 are $\sim$ 49 and $\sim$ 13 emu g^{-1}, respectively. The results show that the bonding of Fe_3O_4 to nano-cellulose/BF_3/Fe_3O_4 causes a decrease in saturation magnetization, but, despite this reduction, the catalyst can still be easily separated from the reaction mixture by using an external magnet with 0.2-T magnetic inductance.

The thermal stability of nano-cellulose/BF_3/Fe_3O_4 was investigated using TGA in the temperature range of 35–770 °C (Fig. 5). The TGA curve illustrates three stages of weight loss. The first weight loss in the range of 95–150 °C (6% weight loss) is related to the removal of moisture from the catalyst. The next weight loss (33%) appears in the range of 263–335 °C and relates to the decomposition of cellulosic units in the nanocomposite. Finally, the main weight loss (60%) is observed in the range of 690–720 °C. The char yield of the catalyst at 770 °C is $\sim$ 78%.

The specific surface area of catalyst was measured by BET theory (Fig. 6). The single point surface area at P/Po = 0.0685 is 65.9890 m^2 g^{-1} and BET surface area is 74.2480 m^2 g^{-1}. The N_2 adsorption isotherm of the catalyst is depicted in Fig. 6a.

After characterization of nano-cellulose/BF_3/Fe_3O_4, the catalytic activity was investigated for the synthesis of 4*H*-pyrimido[2,1-*b*]benzothiazole derivatives via the three-component reaction of aldehydes, 2-amino benzothiazole, and ethyl acetoacetate. In order to optimize the reaction conditions, the model reaction of the 4-nitrobenzaldehyde, 2-amino benzothiazole, and ethyl acetoacetate under various conditions was investigated (Table 2). According to Table 2, the best condition for

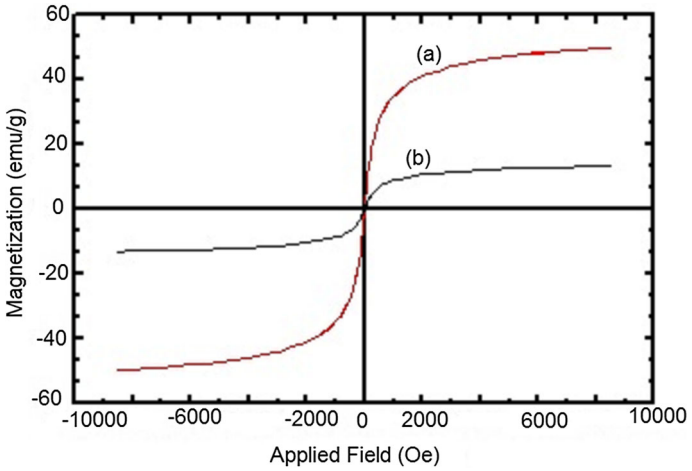

Fig. 4 Magnetization loops of **a** Fe_3O_4 and **b** nano-cellulose/BF_3/Fe_3O_4

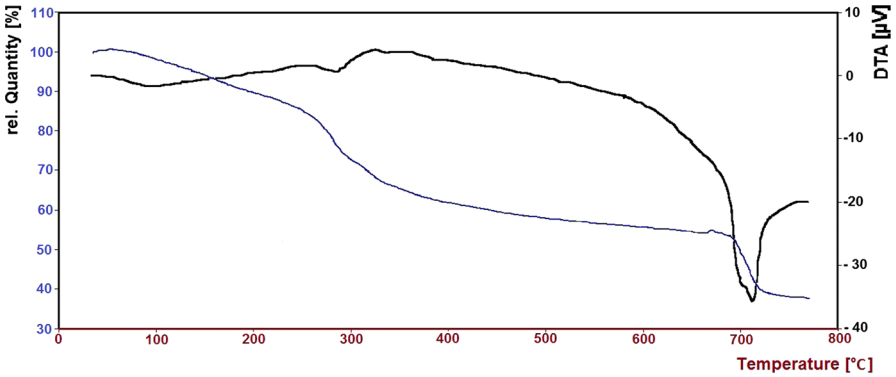

Fig. 5 Thermal gravimetric analysis pattern of nano-cellulose/BF_3/Fe_3O_4

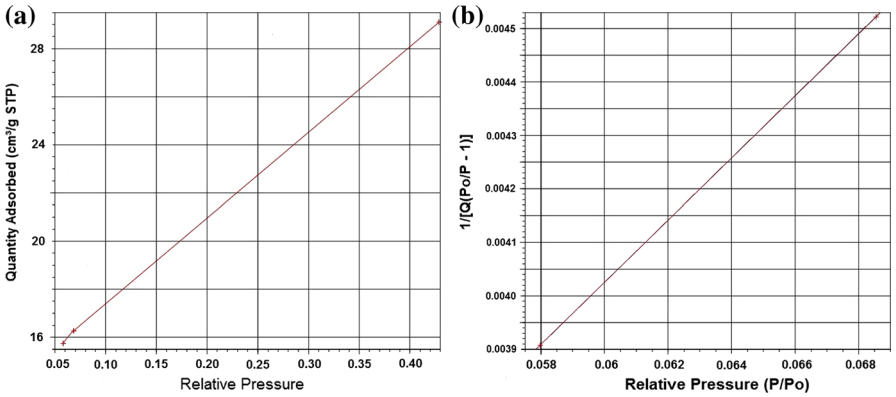

Fig. 6 **a** Nitrogen adsorption isotherms on nano- cellulose/BF_3/Fe_3O_4 and **b** BET of nano-cellulose/BF_3/Fe_3O_4

the reaction is a solvent-free condition using 0.06 g of the catalyst at 100 °C (Table 2, entry 14).

Based on optimal reaction conditions, 4*H*-pyrimido[2,1-*b*]benzothiazole derivatives were synthesized using the three-component condensation of aldehydes (I, 1 mmol), 2-aminobenzothiazole (II, 1 mmol), and ethyl acetoacetate (III, 1 mmol) (Table 3). Electronic effects and the position of the substituent on the aldehyde have considerable effects on the yield and speed of the reaction. Electron-withdrawing groups have higher activity and yield compared to electron-donating groups. The structure of these products was characterized by melting point, FT-IR, and ^{1}H-NMR spectra.

In order to investigate the recoverability and reusability of the catalyst, the above-mentioned model reaction in the presence of nano-cellulose/BF_3/Fe_3O_4 at 100 °C under solvent-free conditions was repeated. After the completion of the reaction, the catalyst was separated by an external magnet and washed several times with dichloromethane and dried at room temperature. The quantity of the recovered

Table 2 The reaction of 4-nitrobenzaldehyde (1 mmol), 2-aminobenzothiazole (1 mmol), and ethyl acetoacetate (1 mmol) in the presence of nano-cellulose/BF_3/Fe_3O_4 under various conditions

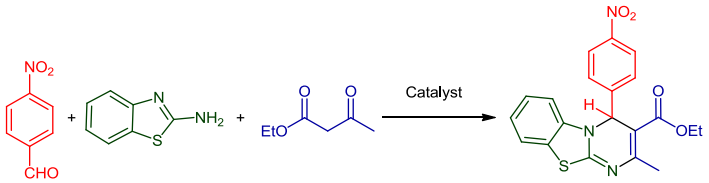

Entry	Solvent	Catalyst (g)	Condition	Time	Yield (%)[a]
1	–	–	R.T.[c]	7 h	–
2	–	–	100 °C	5 h	53
3	–	Fe_3O_4	100 °C	3 h	35
4	–	Fe_3O_4@NCs	100 °C	3 h	38
5	H_2O	Catalyst[b] (0.06)	Reflux	1.8 h	55
6	EtOH	Catalyst[b] (0.06)	Reflux	2 h	40
7	CH_3CN	Catalyst[b] (0.06)	Reflux	2.5 h	43
8	H_2O/EtOH	Catalyst[b] (0.06)	Reflux	2.5 h	50
9	*n*-Hexane	Catalyst[b] (0.06)	Reflux	1.7 h	48
10	CH_3CO_2Et	Catalyst[b] (0.06)	Reflux	3.5 h	45
11	–	Catalyst[b] (0.06)	R.T.[c]	5.3 h	0
12	–	Catalyst[b] (0.06)	80 °C	70 min	68.5
13	–	Catalyst[b] (0.06)	90 °C	60 min	63
14	–	Catalyst[b] (0.06)	100 °C	45 min	98
15	–	Catalyst[b] (0.06)	110 °C	45 min	98
16	–	Catalyst[b] (0.04)	100 °C	70 min	56
17	–	Catalyst[b] (0.05)	100 °C	60 min	78
18	–	Catalyst[b] (0.07)	100 °C	65 min	84

[a]Isolated yield

[b]Nano-cellulose/BF_3/Fe_3O_4

[c]Room temperature

catalyst is 97–99% of the original catalyst weight. The XRD pattern (Fig. 3b) and FTIR (Fig. 1d) of the recovered catalyst show no significant change of its structure under the reaction conditions. The recovered catalyst was then used in the model reaction under the same conditions for four consecutive times without a significant reduction in catalytic activity (Fig. 7).

The proposed mechanism for the synthesis of 4*H*-pyrimido[2,1-*b*]benzothiazoles (IV), is shown in Scheme 2. On the basis of this mechanism, first, ethyl acetoacetate (III) reacts with benzaldehyde (I) according to the Knoevenagel condensation reaction, and then the product thus obtained reacts with 2-aminobenzothiazole (II) through Michael

Table 3 Synthesis of 4*H*-pyrimido[2,1-*b*]benzothiazole derivatives ($IV_{a–l}$) in the presence of nano-cellulose/BF_3/Fe_3O_4 under solvent-free conditions at 100°C

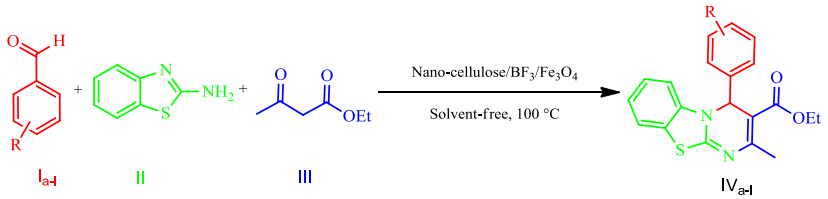

Entry	R	Product	Time (min)	Yield (%)[a]	Melting point, °C [Refs.]
1	H	IV_a	65	80	175–177 [28]
2	4-NO_2	IV_b	45	98	155–157 [28]
3	4-Cl	IV_c	45	92	140–142 [27]
4	4-Br	IV_d	50	97	107–109 [25]
5	4-OH	IV_e	70	92	210–212 [19]
6	3-NO_2	IV_f	60	95	218–220 [31]
7	3-OH	IV_g	75	91	259–261 [32]
8	2-NO_2	IV_h	60	92	170–172
9	2-Cl	IV_i	50	91	125–127 [33]
10	2,4-$(Cl)_2$	IV_j	60	95	104–106
11	2,4-$(OMe)_2$	IV_k	80	85	164–166 [32]
12	3,4-$(OH)_2$	IV_l	75	85	227–229 [31]

The ratio of I (mmol):II (mmol):III (mmol):nano-cellulose/BF_3/Fe_3O_4 (g) is equal to 1:1:1:0.06

[a]Isolated yield

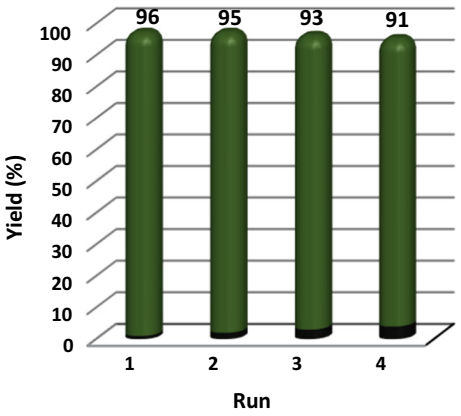

Fig. 7 Catalyst recycling experiments

addition. Subsequently, by cyclization and water removal, 4*H*-pyrimido[2,1-*b*]benzothiazole (IV) derivatives are synthesized. The catalyst used in this reaction acts as a Lewis acid and accelerates the reaction by activating the carbonyl groups.

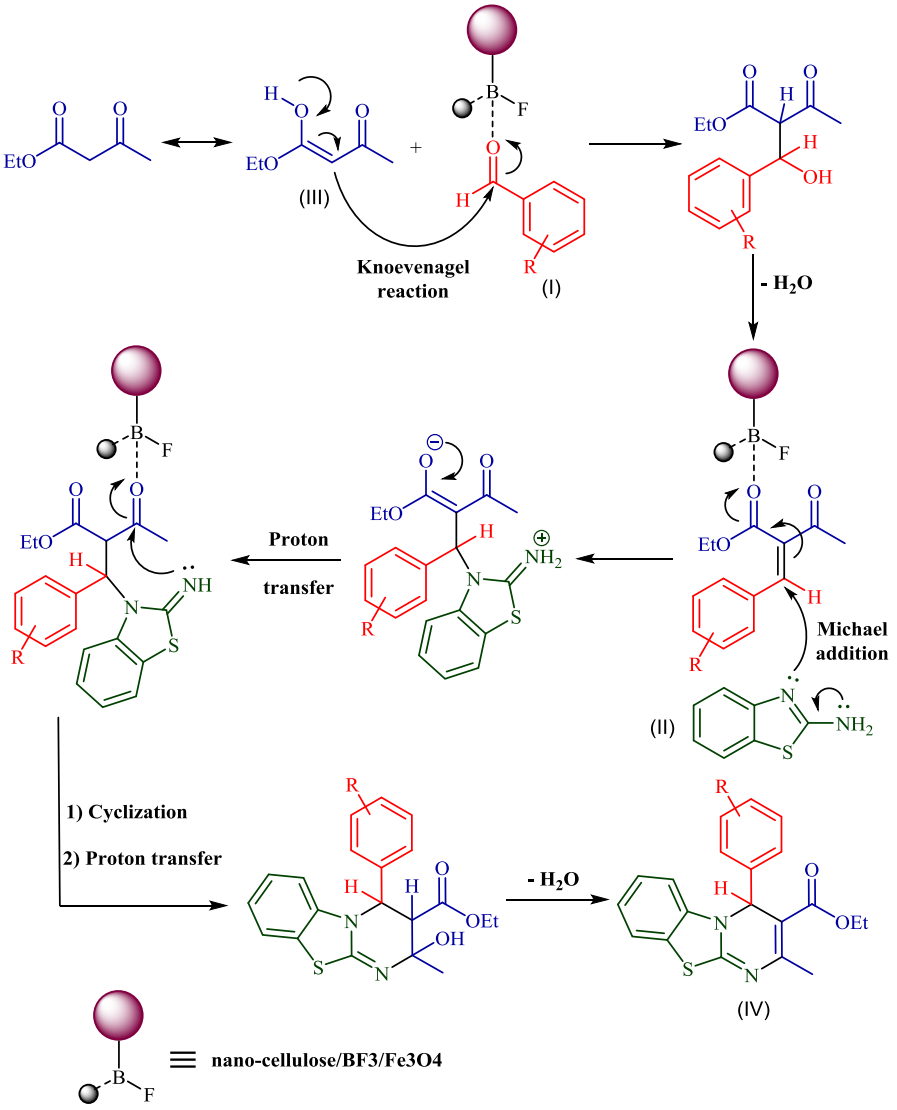

Scheme 2 Proposed mechanism for the synthesis of 4*H*-pyrimido[2,1-*b*]benzothiazole derivatives ($IV_{a–l}$)

The performance of the nano-cellulose/BF_3/Fe_3O_4 catalyst in the model reaction was compared with the other reported catalysts in the synthesis of 4*H*-pyrimido[2,1-*b*]benzothiazole derivatives and the results are summarized in Table 4. The results show that with the nano-cellulose/BF_3/Fe_3O_4 catalyst, 4*H*-pyrimido[2,1-*b*]benzothiazole derivatives can be synthesized in a shorter time and with higher yields. The magnetic property of the catalyst and the greenness of the process are its advantages compared to other catalysts and so are important from an environmental standpoint.

Table 4 Comparison of nano-cellulose/BF_3/Fe_3O_4 catalyst with reported catalysts for the synthesis of 4*H*-pyrimido[2,1-*b*]benzothiazoles

Entry	Catalyst	Condition	Solvent	Time	Yield (%) [Refs.]
1	TMGT[a] (0.08 g)	100 °C	–	5 h	53 [25]
2	TBAHS[b] (30 mol%)	120 °C	Ethylene glycol	2 h	72 [28]
3	Acetic acid (20 mol%)	Reflux	Methanol	18 h	62 [30]
4	$AlCl_3$ (10 mol%)	60–65 °C	–	1.8 h	70 [19]
5	FeF_3 (10 mol%)	80 °C	–	2 h	85 [33]
6	(Mg–Al–CO_3) (0.05 g)	70 °C	–	45 min	79 [34]
7	VB1[c] (10 mol%)	Reflux	Water	75 min	92 [27]
8	Nano-cellulose/BF_3/Fe_3O_4 (0.06)	100 °C	–	45 min	98 [This work]

[a]1,1,3,3-*N*,*N*,*N*′,*N*′-tetramethylguanidinium trifluoroacetate

[b]Tetrabutylammonium hydrogen sulfate

[c]Thiamine hydrochloride

Conclusion

Given the importance of green chemistry, we have reported the synthesis and characterization of nano-cellulose/BF_3/Fe_3O_4 as a bio-based and eco-friendly catalyst with high catalytic activity. It was applied for the synthesis of 4*H*-pyrimido[2,1-*b*]benzothiazole derivatives via the condensation reaction of aromatic aldehydes, 2-aminobenzothiazole, and ethyl acetoacetate. Easy work-up, excellent yield, short reaction time, and reusability of the catalyst are some of the advantages of this novel protocol.

Acknowledgement The Research Council of Yazd University is gratefully acknowledged for the financial support for this work.

References

1. B.M. Reddy, P.M. Sreekanth, P. Lakshmanan, J. Mol. Catal. A Chem. **237**, 93 (2005)
2. J.H. Clark, Acc. Chem. Res. **35**, 791 (2002)
3. N. Lin, A. Dufresne, Eur. Polym. J. **59**, 302 (2014)
4. W.K. Czaja, D.J. Young, M. Kawecki, R.M. Brown, Biomacromolecules **8**, 1 (2007)
5. M. Patchan, J. Graham, Z. Xia, J. Maranchi, R. McCally, O. Schein, J. Elisseeff, M. Trexler, Mater. Sci. Eng. C **33**, 3069 (2013)
6. C. Salas, T. Nypelö, C. Rodriguez-Abreu, C. Carrillo, O.J. Rojas, Curr. Opin. Colloid Interface Sci. **19**, 383 (2014)
7. M. Jorfi, E.J. Foster, J. Appl. Polym. Sci. **132**, 14 (2015)
8. J.O. Zoppe, V. Ruottinen, J. Ruotsalainen, S. Rönkkö, L.-S. Johansson, A. Hinkkanen, K. Järvinen, J. Seppälä, Biomacromolecules **15**, 1534 (2014)
9. M. Kaushik, A. Moores, Green Chem. **18**, 622 (2016)
10. S. Shylesh, V. Schünemann, W.R. Thiel, Angew. Chem. Int. Ed. **49**, 3428 (2010)
11. X. Zheng, S. Luo, L. Zhang, J.-P. Cheng, Green Chem. **11**, 455 (2009)
12. S. Mukherjee, A. Kundu, A. Pramanik, Tetrahedron Lett. **57**, 2103 (2016)

13. M.N. Bhoi, M.A. Borad, E.A. Pithawala, H.D. Patel, Arab. J. Chem. **9** (2016). https://doi.org/10.1016/j.arabjc.2016.01.012
14. M.H. Youssoufi, P.K. Sahu, P.K. Sahu, D.D. Agarwal, M. Ahmad, M. Messali, S. Lahsasni, T.B. Hadda, Med. Chem. Res. **24**, 2381 (2015)
15. R. Ali, N. Siddiqui, J. Chem. **2013**, 1 (2013)
16. M.A. El-Sherbeny, Arzneimittelforschung **50**, 848 (2000)
17. P.K. Sahu, P.K. Sahu, S. Gupta, D. Thavaselvam, D. Agarwal, Eur. J. Med. Chem. **54**, 366 (2012)
18. S. Gupta, N. Ajmera, N. Gautam, R. Sharma, D. Gautam, Indian J. Chem. Sect. B **06**, 853 (2009)
19. P.K. Sahu, P.K. Sahu, J. Lal, D. Thavaselvam, D. Agarwal, Med. Chem. Res. **21**, 3826 (2012)
20. M.T. Gabr, N.S. El-Gohary, E.R. El-Bendary, M.M. El-Kerdawy, Eur. J. Med. Chem. **85**, 576 (2014)
21. J. Yevich, D. Temple Jr., R. Covington, D. Owens, R. Seidehamel, K. Dungan, J. Med. Chem. **25**, 864 (1982)
22. M. Kale, D. Mene, Int. J. Pharma Bio Sci. **4**, 503 (2013)
23. V. Deshmukh, P. Raviprasad, P. Kulkarni, S. Kuberkar, Int. J. Chem. Tech. Res. **3**, 136 (2011)
24. M. Yadav, V.K. Deshmukh, S.R. Chaudhari, Int. J. Pharm. Sci. Rev. Res. **22**, 41 (2013)
25. A. Shaabani, A. Rahmati, S. Naderi, Bioorg. Med. Chem. Lett. **15**, 5553 (2005)
26. A.B. Atar, Y.S. Jeong, Y.T. Jeong, Tetrahedron **70**, 5207 (2014)
27. S.R. Vaidya, J.J. Chamergore, Chem. Biol. Interface **6**, 47 (2016)
28. L. Nagarapu, H.K. Gaikwad, J.D. Palem, R. Venkatesh, R. Bantu, B. Sridhar, Synth. Commun. **43**, 93 (2013)
29. P.K. Sahu, P.K. Sahu, D.D. Agarwal, RSC Adv. **3**, 9854 (2013)
30. P.K. Sahu, P.K. Sahu, Y. Sharma, D.D. Agarwal, J. Heterocycl. Chem. **51**, 1193 (2014)
31. S. Azad, B.B.F. Mirjalili, RSC Adv. **6**, 96928 (2016)
32. S. Azad, B.B.F. Mirjalili, Res. Chem. Intermed. **43**, 3 (2017)
33. A.B. Atar, Y.T. Jeong, Mol. Divers. **18**, 389 (2014)
34. P.K. Sahu, P.K. Sahu, R. Jain, R. Yadav, D.D. Agarwal, Catal. Sci. Technol. **2**, 2465 (2012)